Cationization Effect on the Molecular Weight Distribution of an Ethoxylated Polymer: A Combined Theoretical and Time-of-Flight Secondary Ion Mass Spectroscopic Study

Hansong Cheng,* Paula A. Cornelio Clark, and Scott D. Hanton

Air Products and Chemicals, Inc., 7201 Hamilton Boulevard, Allentown, Pennsylvania 18195-1501

Paul Kung

Molecular Simulations, Inc., 9685 Scranton Road, San Diego, California 92121

Received: October 19, 1999; In Final Form: January 24, 2000

The effect of metal cationization on the molecular weight distribution (MWD) of an ethoxylated polymer, Surfynol 465 (S465), is investigated by time-of-flight secondary ion mass spectrometry (ToF-SIMS) and a hybrid theoretical method combining ab initio density functional theory and molecular mechanics. The MWDs generated from sodium and from silver-cationized oligomers of S465 were measured by ToF-SIMS. The structure and bonding of the cationized complexes were calculated. The results suggest that upon cationization, the metal atoms are chelated by oxygen atoms and, in the case of Ag^+, by the π-orbitals of the C−C triple bond. Although the binding energy of both Na^+ and Ag^+ with the Surfynol molecules is very high for sufficiently long ethoxylate side chains, strong bonding preference is given to Ag^+ over Na^+ due to the orbital interaction between Ag^+ and the Surfynol oligomer via 4d−π* and 5s−π overlap and the ion−dipole interaction between the cations and the oxygen atoms in the ethoxylate chains with Na^+ being of more ionic character. The theoretical results suggest that a minimum ethoxylate chain length is required for Na^+ chelation and that in the high molecular weight region both cations will bind with the Surfynol oligomers strongly, consistent with our experimental observations. We demonstrate that ToF-SIMS is an effective technique for measuring the molecular weight distribution of a low molecular weight oligomer series.

Introduction

Understanding the structure and physicochemical properties of polymeric materials is important in novel materials design. Molecular weight and molecular weight distribution are key fundamental properties of a polymer. Molecular weight directly influences many polymer physical properties.[1] Historically, many different analytical techniques have been used to measure polymer molecular weights. More recently, several mass spectrometry (MS) techniques have been developed which can generate average molecular weight data for relatively low molecular weight synthetic polymers. These techniques rely on a mechanism for volatilization without thermal decomposition and a soft ionization process. Early techniques applicable to polymers include chemical ionization[2,3] and field desorption (FD).[4−8] These require sample heating, however, and chemical ionization is limited to lower molecular weights. In the 1980s, fast atom bombardment[9] was developed and, although applied mostly to biopolymers, found limited application for analysis of polar synthetic polymers with molecular weights below about 3000 Da.[10,11] Recently, the development of electrospray (ESI),[12−16] matrix-assisted laser desorption/ionization (MALDI),[17−21] and static secondary ion mass spectrometry (SIMS)[22−28] have added powerful mass spectral techniques to analyze relatively nonvolatile and labile species.

All synthetic polymers consist of molecules with a distribution of chain lengths.[29] This distribution is characterized by the number-average molecular weight (M_N), the weight-average molecular weight (M_W), and the polydispersity (PD):

$$M_N = \sum M_i N_i / \sum N_i \quad (1)$$

$$M_W = \sum (M_i)^2 N_i / \sum M_i N_i \quad (2)$$

$$\text{polydispersity} = M_W / M_N \quad (3)$$

where M_i is the mass of the ith oligomer in the distribution and N_i is its intensity. These quantities can be calculated from the distribution of observed MS ion peak areas and are useful for comparison of the results. In addition, comparison with other traditional techniques used to investigate polymers, such as size exclusion chromatography (SEC) and nuclear magnetic resonance (NMR) spectroscopy, is important to aid in relating the data produced by the newer techniques to what has been historically accepted.

In previous work,[30] we compared the molecular weight distributions (MWD) for Surfynol 4*XX* (*XX* = 20, 40, 65, and 85), a commercially available series of ethoxylated surfactants, using FAB, MALDI, time-of-flight secondary ion mass spectrometry (ToF-SIMS), and ESI. Figure 1 shows a schematic of a typical ethoxylated Surfynol surfactant. The increasing *XX* values indicate increasing amounts of ethoxylation on a backbone of 2,4,7,9-tetramethyl-5-decyne-4,7-diol. Those experiments demonstrated the ability of probe MS techniques to measure the MWD of various Surfynol surfactants.

In this paper, we report a combined ToF-SIMS and theoretical study on the effect of metal cationization on the MWD of

10.1021/jp9937297 CCC: $19.00
Published on Web 02/29/2000

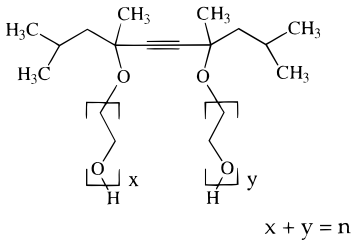

Figure 1. Structure of S4*XX* surfactants. The total ethoxylation, *n*, for a given oligomer is the sum of the ethoxylation, $x + y$, of the two possible sites.

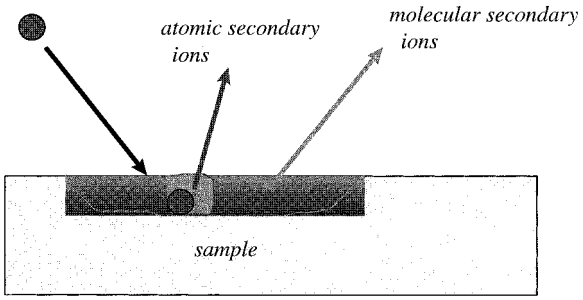

Figure 2. Schematic of SIMS process. The sample is bombarded by a primary ion beam. Atomic and molecular secondary ions are generated as a result of a momentum transfer process.

Surfynol 465 (S465). The MWDs generated from sodium and from silver-cationized oligomers of S465 were measured by ToF-SIMS. Conceptually, SIMS is a very simple technique consisting of a primary ion bombarding step, an energy transfer step, a particle desorption step, and an ion detection step. A schematic depicting the SIMS process is shown in Figure 2. The sample is introduced into an ultrahigh vacuum (UHV) chamber at pressure $\leq 1 \times 10^{-9}$ Torr. The sample is bombarded by a primary ion beam (typically, Xe, Ar, Ga, or Cs ions) accelerated to 5−25 kV. The primary ion impacts the surface and penetrates about 100 Å into the sample. The impact of the primary ion results in an energy and momentum transfer process called the collision cascade. The collision cascade results in the desorption of neutral species and secondary ions from the surface of the sample. The secondary ions are mass analyzed. In static SIMS each sputtering event is thought to originate from a virgin surface and the SIMS spectrum is characteristic of the top few atomic layers.[31,32] The major advantages of SIMS include high sensitivity (ppm detection limits for some elements), the ability to obtain atomic and molecular information, isotopic analysis, lateral characterization (imaging), and analysis of low atomic number elements such as H and Li.[31,33]

After the ToF-SIMS experiments, we carried out theoretical calculations to gain understanding of the structure of S465 and its bonding with the cations. Since the Surfynol molecules usually contain a large number of atoms and conformationally flexible side chains, a full quantum-mechanical calculation is impractical, particularly in view of the large number of conformations involved. We therefore chose a hybrid theoretical method combining quantum-mechanical density functional theory (DFT) and molecular mechanics, which allows us to calculate the structure and energetics of the regions of interest in the molecule accurately by DFT while the rest of the molecule is described adequately by molecular mechanics. The calculated results are then used to explain the observed molecular weight distributions of the oligomers upon cationization. The calculation also yields useful information on the chemical bonding in the cationized oligomeric complexes.

Experiment

For the SIMS experiment, sample solutions of S465 were prepared in methanol at a concentration of 1 mg/mL. Cationization reagent (NaCl or $AgNO_3$) was added to the sample solutions to form saturated solutions. Ten microliters of solution was streamed across a silicon substrate angled at 45°. This sample preparation method yields a thin film in the range of 1−5 monolayers of polymer.

The ToF-SIMS data were collected on a PHI Trift mass spectrometer (Evans East, Plainsboro, NJ, and Charles Evans and Associates, Redwood City, CA). The instrument is equipped with a pulsed, bunched gallium liquid metal ion gun, stigmatic focusing secondary ion optics, and a time-of-flight spectrometer consisting of three sector electrostatic energy analyzers. The data were collected using a 15 kV, bunched gallium primary ion beam, operated at a repetition rate of 5 kHz. The primary ion beam was rastered over a 170 μm × 170 μm area of the sample. The data were collected using ≈3 kV sample potential and 10 kV postacceleration. The primary ion doses did not exceed 10^{12} ions/cm^2 (static SIMS limit). The data were analyzed using Cadence software.

Computational Details

The calculations were done using the QMPOT package,[34] an implementation of the hybrid quantum mechanical/molecular mechanical technique (QM/MM).[35] The hybrid QM/MM methods have been applied to a variety of molecular systems and have been shown to be reasonably accurate and computationally efficient.[36,37] In our hybrid QM/MM calculations, a molecular system is partitioned into QM and MM regions. Appropriate couplings are then set up between the two regions to allow transmission of information such as gradients and charges. In the QM region, the selected atom cluster is treated rigorously using a DFT method powered by the DMol3 package.[38−41] Hydrogen atoms are used to terminate the QM cluster to retain appropriate valence of the terminal atoms. In the MM region, the intramolecular interaction is described by a force field provided by the COMPASS package.[42−46] The total QM/MM energy is calculated by

$$E_{\text{total}}^{\text{QM/MM}} = E_{\text{cluster}}^{\text{QM}} + E_{\text{total}}^{\text{MM}} - E_{\text{cluster}}^{\text{MM}} \qquad (4)$$

where $E_{\text{total}}^{\text{QM/MM}}$ is the total QM/MM energy for the molecule, $E_{\text{cluster}}^{\text{QM}}$ is the QM energy for the cluster only, and $E_{\text{total}}^{\text{MM}}$ and $E_{\text{cluster}}^{\text{MM}}$ are the total energy of the molecule and the cluster energy calculated with molecular mechanics, respectively.

In the DFT calculation, we utilized the GGA functional given by Perdew and Wang[47] with a double numerical basis set augmented with polarization functions. The recently developed COMPASS force field has been tested for a wide variety of organic and organometallic compounds and proven to be reasonably accurate. Full geometry optimization was performed for all the molecular species without a symmetry constraint.

Results and Discussion

ToF-SIMS Mass Spectra and Cationization Effects. Figures 3 and 4 show ToF-SIMS mass spectra of S465 on silicon cationized with Na^+ and Ag^+, respectively. Each mass spectrum shows a series of oligomer ions spaced by 44 D, corresponding to the varying ethoxy chain lengths of the different oligomers. The individual ion masses correspond to the mass of the backbone diol (S104) plus the appropriate number of ethoxy units and the cation. In the ToF-SIMS spectra we see oligomers

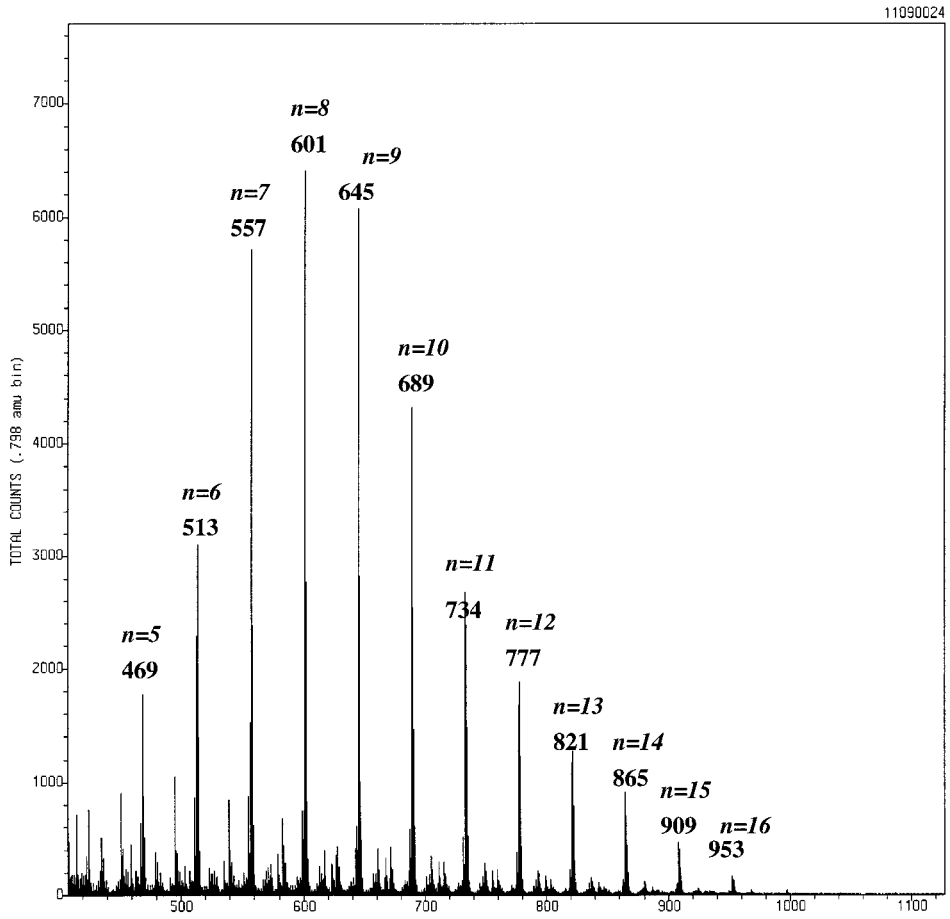

Figure 3. ToF-SIMS spectrum of Surfynol 465/Si cationized by Na^+.

TABLE 1: Molecular Weight of S465 by ToF-SIMS[a]

substrate	cation	M_N	M_W	PD
Si	Ag^+	559	571	1.02
Si	Na^+	638	658	1.03

[a] The precision of the M_N and M_W data is ±7, based upon $n = 9$ measurements.

from about $n = 5$ to about $n = 16$. These data agree well with our previous results for S465.[30]

We have calculated average molecular weight data for these spectra. The molecular weight data is summarized in Table 1. Table 1 indicates that the measured average molecular weights of S465 depend on the metal cation. We obtained higher average molecular weights for Na^+-cationized oligomers than for Ag^+-cationized oligomers. Since the cation is present merely as part of the MS experiment, it is important to understand any impact the choice of the cation has on the ultimately measured MWD. While the differences between the Na^+-cationized and Ag^+-cationized MWDs are small, we wish to understand the mechanism of this observed effect.

To explain the observed differences in the measured molecular weights of S465, we carried out theoretical calculations to understand the interaction of S465 with both Na^+ and Ag^+.

Equilibrium Structures. We will focus on the Surfynol molecule with four ethoxy groups on each side as shown in Figure 5a. This molecule was chosen because its chain lengths are long enough to allow us to examine the effect of both the triple bond and the ethoxy groups on the bonding with cations. Molecules with longer chains are expected to behave in a fashion similar to this one when binding with cations except, perhaps, the binding process may also involve desorption from the substrate. While the detailed process is likely to be more complicated, understanding of the chemical bonding of cations with the relatively shorter side chains will certainly yield useful insight into the driving force that dictates the bonding between the cations and the larger Surfynol oligomers. On the other hand, detailed analysis on the interaction between the cations and the chosen surfactant molecule may also shed light on the interaction between the cations and the shorter chain Surfynol oligomers and help explain the relatively low intensity of short-chain Surfynol oligomers in the ToF-SIMS spectra, particularly in the spectrum of the polymers binding with Na^+, as will be made clear shortly.

We first performed full geometry optimization for the structure. The optimization scheme can be briefly described as follows. First, we speculate that the C−C triple bond might interact with the cations, particularly with Ag^+ via $\pi-5s$ and/or $4d-\pi^*$ orbital overlap. Second, the interaction between the adjacent oxygen atoms with the cations should also be important in determining the bonding. These interactions need to be described accurately. Therefore, we include 10 atoms in the cluster to be calculated quantum-mechanically and the rest of atoms in the molecule are calculated using molecular mechanics. The atoms contained in the quantum cluster are shown with a bold face letter, Q, in Figure 5b. In the case where the Surfynol molecule binds with a cation, the ion was placed at the center of the cluster and was also included in the cluster for quantum-mechanical calculations. Such an arrangement of the initial structure allows the ions to interact with the relevant species in the molecule for efficient geometry optimizations.

We performed systematic conformational search to obtain minimum energy structures of the neutral molecule. While

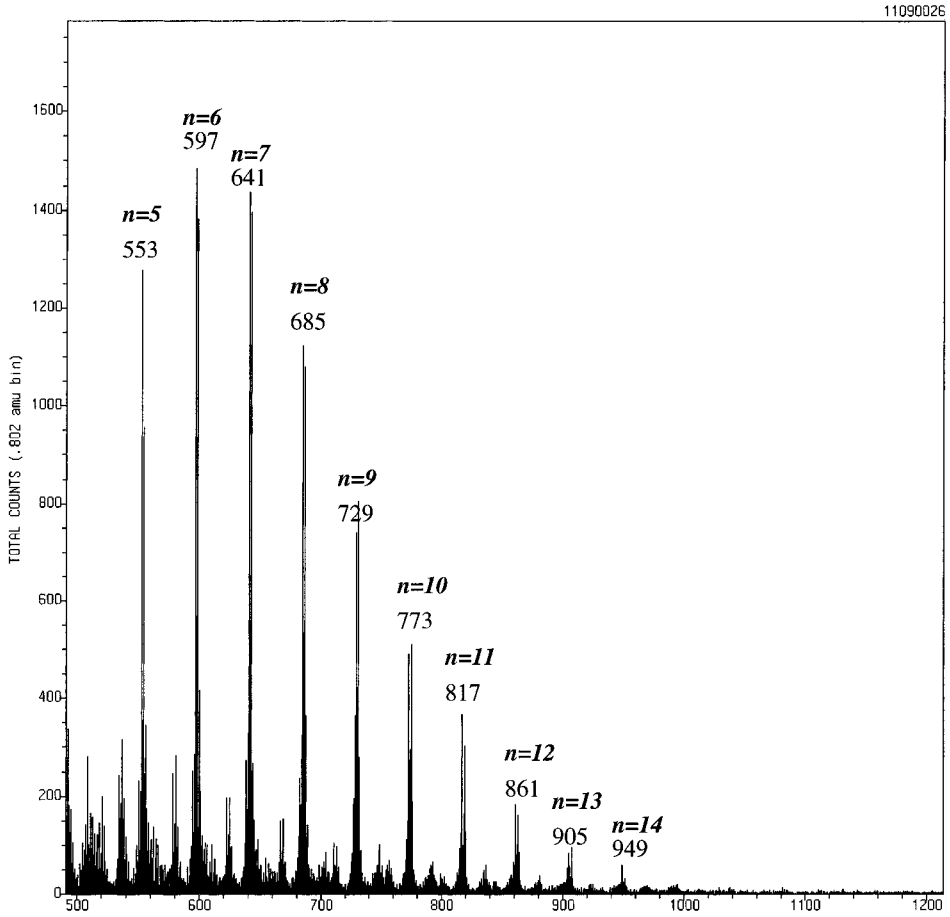

Figure 4. ToF-SIMS spectrum of Surfynol 465/Si cationized by Ag^+.

TABLE 2: Optimized Bond Parameters (Distances in Å and the Angles in deg)

	surfactant	surfactant−Ag^+	surfactant−Na^+
C1−C2	1.476	1.565	1.470
C2−C3	1.218	1.290	1.219
O1−M		2.327	2.521
O2−M		2.339	2.602
O3−M		2.674	2.817
O4−M		2.666	2.821
O5−M		2.826	2.999
O6−M		2.836	3.010
O7−M		4.661	4.802
O8−M		2.722	2.897
C2−M		2.910	2.764
C3−M		2.910	2.775
C1−C2−C3	177.3	159.4	166.4
C4−C3−C2	179.5	159.7	167.3

several conformations with comparable energies were found, the lowest energy conformation for this molecule is the one with two nearly straight chains; at the ends of these chains, the hydroxy groups form a hydrogen bonding to link the chains together with a H-bond distance of 1.709 Å. Some of the key optimized geometric parameters are listed in Table 2. We note from Table 2 that the C−C triple bond is highly rigid with the nearby carbon atoms (C1 and C4) being almost linear with the triple bond. The two long side chains are flexible enough to allow the linkage through the H-bonding without causing a significant energy penalty.

Upon binding with cations, the Surfynol molecule undergoes substantial conformational changes. The fully optimized structure of the [surfactant−Ag]$^+$ complex is shown in Figure 6. The optimized geometry of the complex with Na^+ exhibits similar structure. The key optimized geometric parameters are also shown in Table 2. The side chains, linked by a H-bond but still conformationally flexible, now wrap around the cations similar to the behavior of a typical crown ether compound. The cations are tightly coordinated by seven oxygen atoms. The strength of the O−M^+ (M = Ag or Na) interaction can be readily seen from the bend angles around the C−C triple bond as described by the angles of $C_1-C_2-C_3$ and $C_4-C_3-C_2$, respectively. While the rigidity of the triple bond is manifested in the neutral molecule, the bonds of $C_1-C_2-C_3$ and $C_4-C_3-C_2$ in the compounds containing the metal cations must bend considerably, which gives rise to a significant strain energy in the complexes, to allow bonding between the oxygen atoms and the cations. The bonding between the cation and the oxygen atoms can largely compensate the strain energy, leading to a lower energy conformation. Finally, it is worth noting from Table 2 that the $C_1-C_2-C_3$ and $C_4-C_3-C_2$ bonds in the Ag^+ complex bend much more than those in the Na^+ complex chiefly due to the stronger coordination between Ag^+ and the oxygen atoms.

TABLE 3: Calculated Energy Components (in eV)

	E_{total}^{MM}	$E_{cluster}^{MM}$	$E_{cluster}^{QM}$	E_{total}^{QM-MM}
surf.	−1.9267	−0.0348	−12 615.9323	−12 617.8242
surf. + Ag^+	−5.2512	−0.8494	−15 4120.6637	−15 4125.0655
surf. + Na^+	−3.6665	0.1075	−17027.6666	−17 031.4405
surf. + Na^+	−2.7111	−0.1153	−17 027.6608	−17 030.2567
Ag^+				−14 1502.4697
Na^+				−4410.0598

Energetics and Charge Distribution. The calculated binding energies of the compounds are shown in Table 3, where the energies of the clusters were calculated quantum-mechanically and the rest of the molecules evaluated by molecular mechanics,

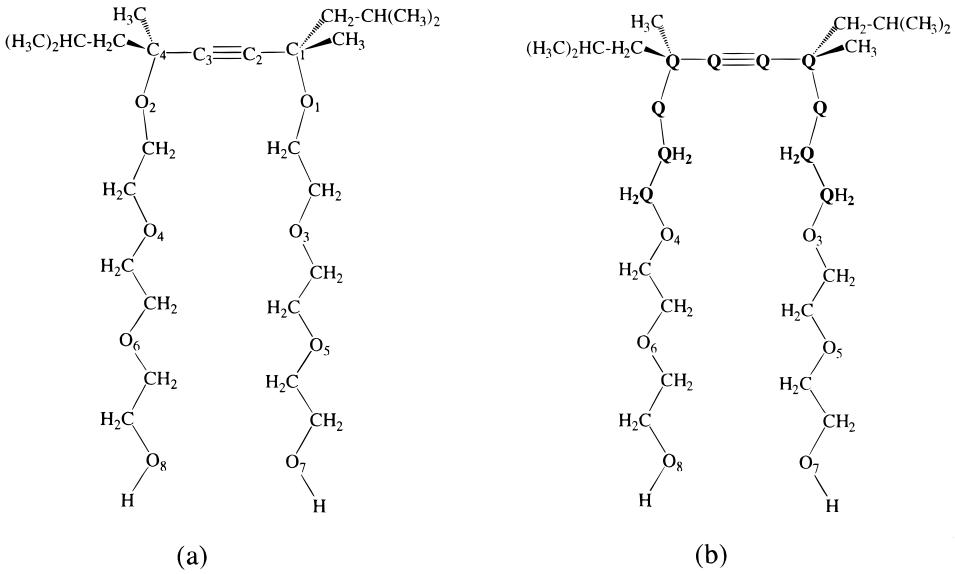

Figure 5. Surfynol molecule used in our QM/MM calculations (a). The atoms contained in the quantum cluster are shown with a bold face letter, Q, in (b).

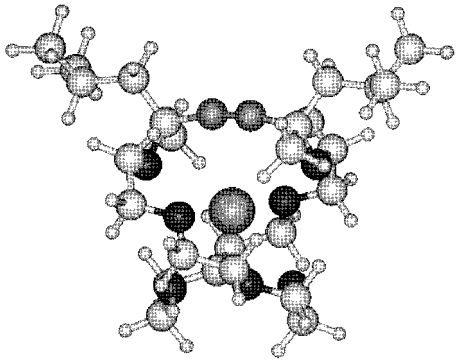

Figure 6. Optimized structure.

TABLE 4: Calculated Mulliken Charges for Selected Atoms in Surfynol Surfactant and Its Complexes with Cations

	surfactant	surfactant−Ag^+	surfactant−Na^+
M		0.608	0.803
C2	−0.056	−0.028	−0.053
C3	−0.059	−0.030	−0.056
O1	−0.473	−0.501	−0.532
O2	−0.472	−0.503	−0.536

as well as the energies of the cations, are also listed. The binding energies of the surfactant molecule with the cations thus can be readily evaluated, which gives −109.99 kcal/mol for Ag^+ and −81.98 for Na^+, respectively. While the surfactant binding with both cations is very strong, the calculation shows considerably strong preference to Ag^+.

Table 4 shows the calculated Mulliken charges for selected atoms in the Surfynol molecule and its complexes with the cations. The relatively larger positive charge on Na suggests a bonding of ionic nature due to its ion−dipole interaction with the Surfynol molecule. On the other hand, the diminished charge on Ag indicates the covalent character of the bonding primarily attributed to the orbital interaction of $\pi \rightarrow$ 5s and 4d $\rightarrow \pi^*$ and to the multicoordination of Ag^+ with seven oxygen atoms.

To understand the contribution to the bonding in the cation−surfactant complexes from various components of the Surfynol molecule, we performed DFT calculations for the complexes of the cations with methyl ether and with acetylene. The results are summarized in Tables 5 and 6, respectively. In the case of methyl ether, we found that the bonding with Ag^+ is about 6.5 kcal/mol stronger than with Na^+, although the binding energy of Na^+ with methyl ether is still substantial. The large positive charge on Na^+ suggests that the bonding between Na^+ and O is indeed of electrostatic nature. The charge transfer from Na^+ to oxygen is only about 0.093. Compared with Na^+, Ag^+ is less ionic when binding with methyl ether with about twice as much charge transferred to oxygen. This gives rise to stronger bonding. For the cation−acetylene complexes, we note that the hydrogen atoms are tilt slightly away from cations as indicated by the calculated H−C−C angle. This is particularly the case with Ag^+ due to its strong orbital interaction with the triple bond. The considerable amount of charge transfer to acetylene suggests strong back-donation from 4d electron of Ag^+ to the π^*-orbital of acetylene, although the π−5s orbital overlap is also important. On the other hand, the ion−induced-dipole interaction in the acetylene-Na^+ complex yields relatively weaker bonding. Consequently, the calculated binding energy of Surfynol molecule with Ag^+ is much larger than the one with Na^+. Both methyl ether and acetylene complexes give stronger binding preference to Ag^+ over Na^+. We also note that the binding energy of Ag^+ with the triple bond in acetylene

TABLE 5: Calculated Binding Energies of Cations M^+ (M = Ag and Na) in Methyl Ether as Well as the Mulliken Charges on the Cations *Q* and the Key Optimized Geometric Parameters

	Ag	Na
ΔE (kcal/mol)	−32.96	−26.49
Q(M)	0.811	0.907
M−O (Å)	2.262	2.206
C−O (Å)	1.454	1.447
C−O−C (deg)	111.8	111.0

TABLE 6: Calculated Binding Energies of Cations M^+ (M = Ag and Na) in Acetylene as Well as the Mulliken Charges on the Cations *Q* and the Key Optimized Geometric Parameters[a]

	Ag	Na
ΔE (kcal/mol)	−29.10	−14.00
Q(M)	0.677	0.875
M−C_c (Å)	2.362	2.621
C−C (Å)	1.223	1.214
H−C−C (deg)	172.1	175.2

[a] C_c stands for the center of mass of the triple bond.

is comparable with the oxygen atom in methyl ether with slight preference to the latter.

The above calculation can be used to explain both the dramatic conformational change of the Surfynol molecule when binding with the cations and its binding preference. In the surfactant−Ag^+ complex, the triple bond must bend considerably despite the strain energy imposed to accommodate the multicoordination between the seven oxygen atoms and the cation. While orbital overlaps between Ag^+ and the triple bond may not be as optimized as in acetylene, the net stabilization energy for Ag^+ by interacting with the oxygen atoms can more than compensate for the loss of orbital interaction energy with the triple bond. The structure shown in Figure 6 also provides an optimal conformation for oxygen atoms to stabilize Na^+.

It is clear from the above analysis that Surfynol oligomers with longer side chains will bind both cations strongly with multicoordinations with oxygen atoms although the preference is given to Ag^+ over Na^+. For short-chain Surfynol oligomers, however, there should be an appreciable difference in the binding energies with the cations. In particular, for a Surfynol molecule with only a hydroxy group on both sides, the ring structure cannot be formed due to the rigidity of the C−C triple bond and the short side chains. Consequently, Na^+ does not interact with the surfactant as effectively as Ag^+ does. In this case, there is even stronger binding preference toward Ag^+ over Na^+. Our previous work indicated that a minimum ethoxylate chain length is required for Na^+ chelation.[30] The Na^+ cationization mechanism discriminates against the very low molecular weight oligomers and produces higher average molecular weights. The stronger binding preference toward Ag^+ over Na^+ indicates that Ag^+ can more effectively cationize the very low molecular weight oligomers of S465. The increased intensity of the low molecular weight oligomers contributes to a lower calculated MWD for Ag^+ than for Na^+ cationization. This is indeed consistent with the observed distribution of low molecular weight oligomers in the ToF-SIMS spectra of S465.

Summary

We have shown in this paper that ToF-SIMS is an effective technique for measuring the molecular weight distribution of an oligomer series. The experiments demonstrated that the measured molecular weight distribution is affected by metal cations, particularly, at the low molecular weight region: Na^+ cationization gives higher M_N and M_W values than Ag^+ cationization. Theoretical calculations based on a hybrid method combining quantum-mechanical density functional theory and molecular mechanics were then performed to understand the interaction between the cations and the Surfynol molecules. The calculation focused on an oligomer with an ethoxylate group of four units on both sides of the C−C triple bond and its complexes with cations.

The fully optimized geometry of the Surfynol molecule exhibits a minimum energy structure with two straight side chains linked by a H-bond at the ends. Upon cationization, however, the two side chains are then folded up to allow the cations to be chelated by oxygen atoms via a multicoordination. As a consequence, the C−C triple bond becomes bent considerably, giving rise to significant strain energy. The calculation yields considerably high binding energies for both Ag^+ and Na^+ in the chelated complexes with strong preference to the former. The primary factors that contribute to the bonding include (1) the orbital interaction between Ag^+ and the C−C triple bond via $4d$-π^* and $5s$-π overlaps, and (2) the ion−dipole interaction between the cations and the oxygen atoms with Na^+ being of more ionic character. In all cases, the interaction between Ag^+ and the Surfynol molecule is stronger than the one between Na^+ and the oligomer.

While a minimum ethoxylate chain length is required for cation chelation due to the rigidity of the C−C triple bond and the insufficient ethoxylate chain length, the improved stability of the Ag^+ cation over the Na^+ cation for the very low molecular weight oligomers results in a lower calculated MWD for the Ag^+-cationized S465. For high molecular weight oligomers, both cations bind strongly with the Surfynol oligomers strongly and thus the relative intensity in the ToF-SIMS spectra essentially remains the same.

Acknowledgment. The authors thank Air Products and Chemicals, Inc. for its support of this research, Dr. David Parees for helpful discussions about the ToF-SIMS data, Drs. Patricia L. Lindley of Charles Evans & Associates and David A. Cole of Evans East for assisting in data collection, and Drs. Bob Coraor and Tom Mebrahtu for critical review of the manuscript. We also thank Dr. Amitesh Maiti of Molecular Simulations Inc. for helpful discussions about the QM/MM work.

References and Notes

(1) Sperling, L. H. *Introduction to Physical Polymer Science*; John Wiley & Sons: New York, 1986.
(2) Smith, R. D.; Fjeldsted, J.; Lee M. L. *Int. J. Mass Spectrom. Ion Phys.* **1983**, *46*, 217.
(3) Vincenti, M.; Pelizzetti, E.; Guarini, A.; Costanzi, S. *Anal. Chem.* **1992**, *64*, 1879.
(4) Prokai, L. *Field Desorption Mass Spectrometry*; Marcel Dekker: New York, 1990.
(5) Lattimer, R. P.; Harmon, D. J.; Welch, K. R. *Anal. Chem.* **1979**, *51*, 1293.
(6) Scrivens, J. H.; Jennings, R. C. K. J.; Yates, H.; Taylor, M. J.; Jackson, A. *Proc. 42nd ASMS Conf. Mass Spectrom. Allied Top., Chicago, IL* **1994**, 313.
(7) Saito, J.; Toda, S.; Tanaka, S. *Bunseki Kagaku* **1980**, *29*, 462.
(8) Oshiro, H.; Sato, J.; Shimada, M. *Kanzei Chuo Bunsekishoho* **1986**, *26*, 23.
(9) Barber, M.; Bordoli, R.; Sedgwick, R. D.; Tyler, A. N. J. *J. Chem. Soc., Chem. Commun.* **1981**, 325.
(10) Facino, R. M.; Carini, M.; Minghetti, P.; Moneti, G.; Arlandini, E.; Melis, S. *Biomed. Environ. Mass Spectrom.* **1989**, *18*, 673.
(11) Seraglia, R.; Traldi, P.; Mendichi, R.; Sartore, L.; Schiavon, O.; Veronese, R. M. *Anal. Chim. Acta* **1992**, *262*, 277.
(12) Fenn, J. B. *J. Am. Soc. Mass Spectrom.* **1993**, *4*, 524.
(13) Yamashita, M.; Fenn, J. B. *J. Phys. Chem.* **1984**, *88*, 4451.
(14) Yamashita, M.; Fenn, J. B. *J. Phys. Chem.* **1984**, *88*, 4471.
(15) Fenn, J. B.; Mann, M.; Meng, C. K.; Wong, S. F.; Whitehouse, C. M. *Science* **1989**, *246*, 64.
(16) Dole, M.; Mack, L. L.; Hines, R. L.; Mobley, R. C.; Ferguson, L. D.; Alice, M. B. *J. Chem. Phys.* **1968**, *49*, 2240.
(17) Tanaka, K.; Waki, H.; Ido, Y.; Akita, S.; Yoshida, Y.; Yoshida, T. *Rapid Commun. Mass Spectrom.* **1988**, *2*, 151.
(18) Karas, M.; Hillenkamp, F. *Anal. Chem.* **1988**, *60*, 2299.
(19) Bahr, U.; Deppe, A.; Karas, M.; Hillenkamp, F.; Giessman, U. *Anal. Chem.* **1992**, *64*, 2866.
(20) Danis, P.; Karr, D.; Mayer, F.; Holle, A.; Watson, C. *Org. Mass Spectrom.* **1992**, *27*, 843.
(21) Danis, P.; Karr, D. *Org. Mass Spectrom.* **1993**, *28*, 923.
(22) Benninghoven, A. *Angew. Chem., Int. Ed. Engl.* **1994**, *33*, 1023.
(23) Bletsos, I. V.; Hercules, D. M.; van Leyen, D.; Benninghoven, A. *Macromolecules* **1987**, *20*, 407.
(24) Benninghoven, A. *Angew Chem., Int. Ed. Engl.* **1994**, *33*, 1023.
(25) Pachuta, S. J.; Cooks, R. G. *Chem. Rev.* **1987**, *87*, 647.
(26) Wandass, J. H.; Schmitt, R. L.; Gardella, Jr., J. A. *J. Appl. Surf. Sci.* **1989**, *40*, 85.
(27) Grade, H.; Winograd, N.; Cooks, R. G. *J. Am. Chem. Soc.* **1977**, *99*, 7725.
(28) Benninghoven, A.; Rudenauer, F. G.; Werner, H. W. *Secondary Ion Mass Spectrometry—Basic Concepts, Instrumental Aspects, Applications and Trends*; John Wiley & Sons: New York, 1987.
(29) Rosen, S. L. *Fundamental Principles of Polymeric Materials*; John Wiley & Sons: New York, 1982; Chapter 6.
(30) Parees, D. M.; Hanton, S. D.; Cornelio Clark, P. A.; Willcox, D. A. *J. Am. Soc. Mass Spectrom.* **1998**, *9*, 282.

(31) Benninghoven, A.; Ruedenauer, F. G.; Werner, H. W. *Secondary Ion Mass Spectrometry*; John Wiley and Sons: New York, 1987.
(32) Hercules, D. M.; Hercules, S. H. *J. Chem. Educ.* **1984**, *61*, 593.
(33) Benninghoven, A. *Int. J. Mass Spectrom. Ion Phys*. **1983**, *53*, 85.
(34) QMPOT, version 1.5 beta; Molecular Simulations, Inc., 1998.
(35) Eichler, U.; Kölmel, C. M.; Sauer, J. *J. Comput. Chem.* **1996**, *18*, 463.
(36) Brändle, M.; Sauer, J. *J. Am. Chem. Soc.* **1998**, *120*, 1556.
(37) Rodriguez-Santiago, L.; Sierka, M.; Branchadell, V.; Sodupe, M.; Sauer, J. *J. Am. Chem. Soc.* **1998**, *120*, 1545.
(38) DMol^3, version 3.9; Molecular Simulations, Inc., 1998.
(39) Delley, B. *J. Chem. Phys.* **1990**, *92*, 508.
(40) Delley, B. *J. Chem. Phys.* **1991**, *94*, 7245.
(41) Delley, B. In *Density Functional Theory: A Tool for Chemistry*; Seminario, J., Politzer, P., Eds.; Elsevier: Amsterdam, 1995.
(42) COMPASS; Molecular Simulations Inc., 1998.
(43) Sun, H *J. Phys. Chem. B* **1998**, *102*, 7338.
(44) Sun, H.; Rigby, D. *Spectrochim. Acta, Part A* **1997**, *53*, 1301.
(45) Rigby, D.; Sun, H.; Eichinger, B. E. *Polym. Int.* **1997**, *44*, 311.
(46) Sun, H.; Fried, J. R.; Ren, P. *Comput. Theor. Polym. Sci.*, in press.
(47) Perdew, J. P.; Wang, Y. *Phys. Rev B* **1992**, *45*, 13244.